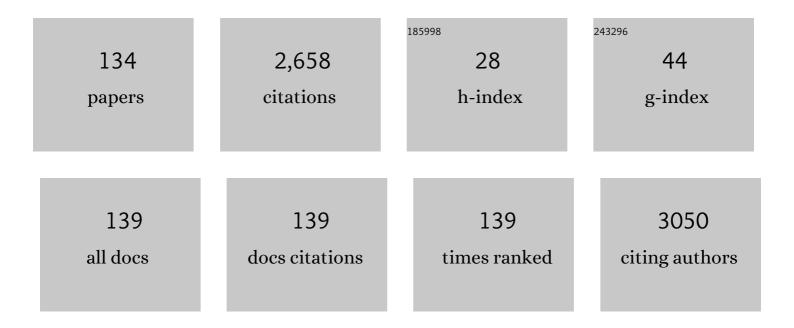
Eva Forssell-Aronsson

List of Publications by Year in descending order

Source: https://exaly.com/author-pdf/6012429/publications.pdf Version: 2024-02-01



#	Article	IF	CITATIONS
1	Hyperfractionated Treatment with 177Lu-Octreotate Increases Tumor Response in Human Small-Intestine Neuroendocrine GOT1 Tumor Model. Cancers, 2022, 14, 235.	1.7	1
2	Age-related long-term response in rat thyroid tissue and plasma after internal low dose exposure to 1311. Scientific Reports, 2022, 12, 2107.	1.6	0
3	Natural radioactivity and element characterization in pit lakes in Northern Sweden. PLoS ONE, 2022, 17, e0266002.	1.1	1
4	Age and sex effects across the blood proteome after ionizing radiation exposure can bias biomarker screening and risk assessment. Scientific Reports, 2022, 12, 7000.	1.6	4
5	Effects of different mean arterial pressure targets on plasma volume, ANP and glycocalyx—A randomized trial. Acta Anaesthesiologica Scandinavica, 2021, 65, 220-227.	0.7	8
6	Genetic alterations associated with multiple primary malignancies. Cancer Medicine, 2021, 10, 4465-4477.	1.3	7
7	Neuroblastoma xenograft models demonstrate the therapeutic potential of 177Lu-octreotate. BMC Cancer, 2021, 21, 950.	1.1	4
8	Neurochemical properties measured by 1H magnetic resonance spectroscopy may predict cognitive behaviour therapy outcome in paediatric OCD: a pilot study. Journal of Neural Transmission, 2021, 128, 1361-1370.	1.4	2
9	VERDICT MRI for radiation treatment response assessment in neuroendocrine tumors. NMR in Biomedicine, 2021, , e4680.	1.6	0
10	Genomic profiling of the transcription factor Zfp148 and its impact on the p53 pathway. Scientific Reports, 2020, 10, 14156.	1.6	5
11	Increased therapeutic effect on medullary thyroid cancer using a combination of radiation and tyrosine kinase inhibitors. PLoS ONE, 2020, 15, e0233720.	1.1	2
12	The IRI-DICE hypothesis: ionizing radiation-induced DSBs may have a functional role for non-deterministic responses at low doses. Radiation and Environmental Biophysics, 2020, 59, 349-355.	0.6	1
13	Optimization of cell viability assays to improve replicability and reproducibility of cancer drug sensitivity screens. Scientific Reports, 2020, 10, 5798.	1.6	106
14	Long-term transcriptomic and proteomic effects in Sprague Dawley rat thyroid and plasma after internal low dose 1311 exposure. PLoS ONE, 2020, 15, e0244098.	1.1	7
15	Title is missing!. , 2020, 15, e0233720.		0
16	Title is missing!. , 2020, 15, e0233720.		0
17	Title is missing!. , 2020, 15, e0233720.		0

#	Article	IF	CITATIONS
19	Protection of Kidney Function with Human Antioxidation Protein α ₁ -Microglobulin in a Mouse ¹⁷⁷ Lu-DOTATATE Radiation Therapy Model. Antioxidants and Redox Signaling, 2019, 30, 1746-1759.	2.5	22
20	Gemcitabine potentiates the anti-tumour effect of radiation on medullary thyroid cancer. PLoS ONE, 2019, 14, e0225260.	1.1	7
21	Transcriptional effects of 177Lu-octreotate therapy using a priming treatment schedule on GOT1 tumor in nude mice. EJNMMI Research, 2019, 9, 28.	1.1	3
22	Multiparametric MR for nonâ€invasive evaluation of tumour tissue histological characteristics after radionuclide therapy. NMR in Biomedicine, 2019, 32, e4060.	1.6	12
23	Dataâ€driven identification of tumor subregions based on intravoxel incoherent motion reveals association with proliferative activity. Magnetic Resonance in Medicine, 2019, 82, 1480-1490.	1.9	5
24	Local treatment of liver metastases by administration of 177Lu-octreotate via isolated hepatic perfusion – A preclinical simulation of a novel treatment strategy. Surgical Oncology, 2019, 29, 148-156.	0.8	0
25	177Lu-octreotate therapy for neuroendocrine tumours is enhanced by Hsp90 inhibition. Endocrine-Related Cancer, 2019, 26, 437-449.	1.6	14
26	Time-dependent transcriptional response of GOT1 human small intestine neuroendocrine tumor after 177Lu[Lu]-octreotate therapy. Nuclear Medicine and Biology, 2018, 60, 11-18.	0.3	7
27	Identification of Potential MR-Derived Biomarkers for Tumor Tissue Response to 177Lu-Octreotate Therapy in an Animal Model of Small Intestine Neuroendocrine Tumor. Translational Oncology, 2018, 11, 193-204.	1.7	9
28	[OA166] A1M is a potential kidney protector in 177Lu-octreotate treatment of neuroendocrine tumours. Physica Medica, 2018, 52, 63-64.	0.4	0
29	[OA164] Vandetanib may act as a radiosensitiser for 177Lu-octreotate treatment of medullary thyroid cancer. Physica Medica, 2018, 52, 62-63.	0.4	0
30	Deconvolution of expression microarray data reveals 1311-induced responses otherwise undetected in thyroid tissue. PLoS ONE, 2018, 13, e0197911.	1.1	5
31	Clonal relatedness in tumour pairs of breast cancer patients. Breast Cancer Research, 2018, 20, 96.	2.2	14
32	Estimation of tumour volume at therapy initiation by back-extrapolating the post-therapy regression curve of tumour volume. Applied Cancer Research, 2018, 38, .	1.0	1
33	Genome-wide multi-omics profiling of the 8p11-p12 amplicon in breast carcinoma. Oncotarget, 2018, 9, 24140-24154.	0.8	19
34	¹ H magnetic resonance spectroscopy evidence for occipital involvement in treatment-naive paediatric obsessive–compulsive disorder. Acta Neuropsychiatrica, 2017, 29, 179-190.	1.0	8
35	Microarray Studies on 211At Administration in BALB/c Nude Mice Indicate Systemic Effects on Transcriptional Regulation in Nonthyroid Tissues. Journal of Nuclear Medicine, 2017, 58, 346-353.	2.8	10
36	A Novel 18-Marker Panel Predicting Clinical Outcome in Breast Cancer. Cancer Epidemiology Biomarkers and Prevention, 2017, 26, 1619-1628.	1.1	1

#	Article	IF	CITATIONS
37	The influence of cardiac triggering time and an optimization strategy for improved cardiac MR spectroscopy. Zeitschrift Fur Medizinische Physik, 2017, 27, 310-317.	0.6	2
38	Priming increases the anti-tumor effect and therapeutic window of 177Lu-octreotate in nude mice bearing human small intestine neuroendocrine tumor GOT1. EJNMMI Research, 2017, 7, 6.	1.1	16
39	Evaluation of two intraoperative gamma detectors for assessment of 177Lu activity concentration in vivo. EJNMMI Physics, 2017, 4, 3.	1.3	1
40	NAMPT Inhibitor GMX1778 Enhances the Efficacy of ¹⁷⁷ Lu-DOTATATE Treatment of Neuroendocrine Tumors. Journal of Nuclear Medicine, 2017, 58, 288-292.	2.8	33
41	Hedgehog inhibitor sonidegib potentiates 177Lu-octreotate therapy of GOT1 human small intestine neuroendocrine tumors in nude mice. BMC Cancer, 2017, 17, 528.	1.1	24
42	Transcriptional response to 1311 exposure of rat thyroid gland. PLoS ONE, 2017, 12, e0171797.	1.1	10
43	Non-targeted transcriptomic effects upon thyroid irradiation: similarity between in-field and out-of-field responses varies with tissue type. Scientific Reports, 2016, 6, 30738.	1.6	7
44	Linking loss of sodium-iodide symporter expression to DNA damage. Experimental Cell Research, 2016, 344, 120-131.	1.2	8
45	The amount of injected 177Lu-octreotate strongly influences biodistribution and dosimetry in C57BL/6N mice. Acta Oncológica, 2016, 55, 68-76.	0.8	7
46	Circadian rhythm influences genome-wide transcriptional responses to 1311 in a tissue-specific manner in mice. EJNMMI Research, 2015, 5, 75.	1.1	12
47	Transcriptional Response in Mouse Thyroid Tissue after 211At Administration: Effects of Absorbed Dose, Initial Dose-Rate and Time after Administration. PLoS ONE, 2015, 10, e0131686.	1.1	12
48	Gene expression signature in mouse thyroid tissue after 1311 and 211At exposure. EJNMMI Research, 2015, 5, 59.	1.1	13
49	Dose-specific transcriptional responses in thyroid tissue in mice after 1311 administration. Nuclear Medicine and Biology, 2015, 42, 263-268.	0.3	19
50	Renal function affects absorbed dose to the kidneys and haematological toxicity during 177Lu-DOTATATE treatment. European Journal of Nuclear Medicine and Molecular Imaging, 2015, 42, 947-955.	3.3	79
51	Transcriptional response in normal mouse tissues after i.v. 211At administration - response related to absorbed dose, dose rate, and time. EJNMMI Research, 2015, 5, 1.	1.1	46
52	Potential Biomarkers for Radiation-Induced Renal Toxicity following 177Lu-Octreotate Administration in Mice. PLoS ONE, 2015, 10, e0136204.	1.1	12
53	Evaluation of retinol binding protein 4 and carbamoylated haemoglobin as potential renal toxicity biomarkers in adult mice treated with 177Lu-octreotate. EJNMMI Research, 2014, 4, 59.	1.1	3
54	Time- and dose rate-related effects of internal 177Lu exposure on gene expression in mouse kidney tissue. Nuclear Medicine and Biology, 2014, 41, 825-832.	0.3	19

#	Article	IF	CITATIONS
55	Additive effect of the AZGP1, PIP, S100A8 and UBE2C molecular biomarkers improves outcome prediction in breast carcinoma. International Journal of Cancer, 2014, 134, 1617-1629.	2.3	57
56	Dosimetric analysis of 123I, 125I and 131I in thyroid follicle models. EJNMMI Research, 2014, 4, 23.	1.1	8
57	Analysis of inter-patient variations in tumour growth rate. Theoretical Biology and Medical Modelling, 2014, 11, 21.	2.1	9
58	Transcriptional response of kidney tissue after 177Lu-octreotate administration in mice. Nuclear Medicine and Biology, 2014, 41, 238-247.	0.3	14
59	Distinct microRNA Expression Profiles in Mouse Renal Cortical Tissue after 177Lu-octreotate Administration. PLoS ONE, 2014, 9, e112645.	1.1	5
60	A new method to estimate parameters of the growth model for metastatic tumours. Theoretical Biology and Medical Modelling, 2013, 10, 31.	2.1	12
61	Biodistribution and Dosimetry of Free ²¹¹ At, ¹²⁵ I ^{â^'} and ¹³¹ I ^{â^'} in Rats. Cancer Biotherapy and Radiopharmaceuticals, 2013, 28, 657-664.	0.7	62
62	Radionuclide Therapy via SSTR: Future Aspects from Experimental Animal Studies. Neuroendocrinology, 2013, 97, 86-98.	1.2	20
63	Gastrointestinal stromal tumors (GISTs) express somatostatin receptors and bind radiolabeled somatostatin analogs. Acta Oncológica, 2013, 52, 783-792.	0.8	16
64	Comparative Analysis of Transcriptional Gene Regulation Indicates Similar Physiologic Response in Mouse Tissues at Low Absorbed Doses from Intravenously Administered 211At. Journal of Nuclear Medicine, 2013, 54, 990-998.	2.8	27
65	Nephrotoxicity profiles and threshold dose values for [177Lu]-DOTATATE in nude mice. Nuclear Medicine and Biology, 2012, 39, 756-762.	0.3	34
66	Estimation of absorbed dose to the kidneys in patients after treatment with 177Lu-octreotate: comparison between methods based on planar scintigraphy. EJNMMI Research, 2012, 2, 49.	1.1	52
67	Transcriptional response of BALB/c mouse thyroids following in vivo astatine-211 exposure reveals distinct gene expression profiles. EJNMMI Research, 2012, 2, 32.	1.1	30
68	Microdosimetric analysis of 211At in thyroid models for man, rat and mouse. EJNMMI Research, 2012, 2, 29.	1.1	8
69	Tumour size measurement in a mouse model using high resolution MRI. BMC Medical Imaging, 2012, 12, 12.	1.4	38
70	Inhomogeneous activity distribution of 177Lu-DOTA0-Tyr3-octreotate and effects on somatostatin receptor expression in human carcinoid GOT1 tumors in nude mice. Tumor Biology, 2012, 33, 229-239.	0.8	6
71	Advances in the diagnostic imaging of pheochromocytomas. Reports in Medical Imaging, 2011, , 19.	0.8	6
72	Binding of TS1, an anti-keratin 8 antibody, in small-cell lung cancer after 177Lu-DOTA-Tyr3-octreotate treatment: a histological study in xenografted mice. EJNMMI Research, 2011, 1, 19.	1.1	7

#	Article	IF	CITATIONS
73	Effects of internal low-dose irradiation from 131I on gene expression in normal tissues in Balb/c mice. EJNMMI Research, 2011, 1, 29.	1.1	24
74	Biodistribution of 177Lu-octreotate and 111In-minigastrin in female nude mice transplanted with human medullary thyroid carcinoma GOT2. Oncology Reports, 2011, 27, 174-81.	1.2	17
75	Radiation Induces Up-Regulation of Somatostatin Receptors 1, 2, and 5 in Small Cell Lung Cancer <i>In Vitro</i> Also at Low Absorbed Doses. Cancer Biotherapy and Radiopharmaceuticals, 2011, 26, 759-765.	0.7	15
76	[¹⁷⁷ Luâ€DOTA ⁰ â€Tyr ³]â€Octreotate Treatment in Patients with Disseminated Gastroenteropancreatic Neuroendocrine Tumors: The Value of Measuring Absorbed Dose to the Kidney. World Journal of Surgery, 2010, 34, 1368-1372.	0.8	62
77	New Medical Strategies for Midgut Carcinoids. Anti-Cancer Agents in Medicinal Chemistry, 2010, 10, 250-269.	0.9	8
78	Anterior to posterior hippocampal MRS metabolite difference is mainly a partial volume effect. Acta Radiologica, 2010, 51, 351-359.	0.5	4
79	Radiation-Induced Thyroid Stunning: Differential Effects of 123I, 131I, 99mTc, and 211At on Iodide Transport and NIS mRNA Expression in Cultured Thyroid Cells. Journal of Nuclear Medicine, 2009, 50, 1161-1167.	2.8	44
80	Comparison of Electron Dose-Point Kernels in Water Generated by the Monte Carlo Codes, PENELOPE, GEANT4, MCNPX, and ETRAN. Cancer Biotherapy and Radiopharmaceuticals, 2009, 24, 461-467.	0.7	31
81	Quantitative analysis of tumor growth rate and changes in tumor marker level: Specific growth rate versus doubling time. Acta Oncológica, 2009, 48, 591-597.	0.8	35
82	A 1H magnetic resonance spectroscopy study in adults with obsessive compulsive disorder: relationship between metabolite concentrations and symptom severity. Journal of Neural Transmission, 2008, 115, 1051-1062.	1.4	82
83	Tumour control probability (TCP) for non-uniform activity distribution in radionuclide therapy. Physics in Medicine and Biology, 2008, 53, 4369-4381.	1.6	10
84	Comparison of [¹⁷⁷ Lu-DOTA ⁰ ,Tyr ³]-Octreotate and [¹⁷⁷ Lu-DOTA ⁰ ,Tyr ³]-Octreotide for Receptor-Mediated Radiation Therapy of the Xenografted Human Midgut Carcinoid Tumor GOT1. Cancer Biotherapy and Radiopharmaceuticals, 2008, 23, 114-120.	0.7	22
85	Specific Growth Rate versus Doubling Time for Quantitative Characterization of Tumor Growth Rate. Cancer Research, 2007, 67, 3970-3975.	0.4	200
86	Effects of Treatment with 177Lu-DOTA-Tyr3-Octreotate on Uptake of Subsequent Injection in Carcinoid-Bearing Nude Mice. Cancer Biotherapy and Radiopharmaceuticals, 2007, 22, 644-653.	0.7	22
87	Down-regulation of the Sodium/Iodide Symporter Explains 131I-Induced Thyroid Stunning. Cancer Research, 2007, 67, 7512-7517.	0.4	53
88	Transport of free 211At and 1251â°' in thyroid epithelial cells: effects of anion channel blocker 4,4′-diisothiocyanostilbene-2,2′-disulfonic acid on apical efflux and cellular retention. Nuclear Medicine and Biology, 2007, 34, 523-530.	0.3	7
89	Translation of Dosimetric Results of Preclinical Radionuclide Therapy to Clinical Situations: Influence of Photon Irradiation. Cancer Biotherapy and Radiopharmaceuticals, 2007, 22, 268-274.	0.7	6
90	Reduced iodide transport (stunning) and DNA synthesis in thyrocytes exposed to low absorbed doses from 1311 in vitro. Journal of Nuclear Medicine, 2007, 48, 481-6.	2.8	19

#	Article	IF	CITATIONS
91	Radiation-induced up-regulation of somatostatin receptor expression in small cell lung cancer in vitro. Nuclear Medicine and Biology, 2006, 33, 841-846.	0.3	34
92	Biodistribution of Free 211At and 125l– in Nude Mice Bearing Tumors Derived from Anaplastic Thyroid Carcinoma Cell Lines. Cancer Biotherapy and Radiopharmaceuticals, 2006, 21, 591-600.	0.7	26
93	Can Quantification of VMAT and SSTR Expression Be Helpful for Planning Radionuclide Therapy of Malignant Pheochromocytomas?. Annals of the New York Academy of Sciences, 2006, 1073, 491-497.	1.8	24
94	Aspects on Radionuclide Therapy in Malignant Pheochromocytomas. Annals of the New York Academy of Sciences, 2006, 1073, 498-504.	1.8	6
95	Malignant Pheochromocytoma in a Population-Based Study: Survival and Clinical Results. Annals of the New York Academy of Sciences, 2006, 1073, 512-516.	1.8	22
96	Dosimetric characterization of radionuclides for systemic tumor therapy: Influence of particle range, photon emission, and subcellular distribution. Medical Physics, 2006, 33, 3260-3269.	1.6	40
97	Electron- and positron-emitting radiolanthanides for therapy: aspects of dosimetry and production. Journal of Nuclear Medicine, 2006, 47, 807-14. Adsorption and volatility of free 211At and 125 <mml:math <="" altimg="si53.gif" overflow="scroll" td=""><td>2.8</td><td>56</td></mml:math>	2.8	56
98	xmlns:xocs="http://www.elsevier.com/xml/xocs/dtd" xmlns:xs="http://www.w3.org/2001/XMLSchema" xmlns:xsi="http://www.w3.org/2001/XMLSchema-instance" xmlns="http://www.elsevier.com/xml/ja/dtd" xmlns:ja="http://www.elsevier.com/xml/ja/dtd" xmlns:mml="http://www.w3.org/1998/Math/MathML" xmlns:tb="http://www.elsevier.com/xml/common/table/dtd"	0.7	12
99	xmlns:sb="http://www.elsevier.com/xml/common/struct-bib/dtd" xmlns:ce="http://w. Applied Radiation A Novel Photon Radiation Detector System for In Vitro Biokinetic Measurements. Cancer Biotherapy and Radiopharmaceuticals, 2005, 20, 629-638.	0.7	0
100	Differences in Biodistribution Between 99mTc-Depreotide, 111In-DTPA-Octreotide, and 177Lu-DOTA-Tyr3-Octreotate in a Small Cell Lung Cancer Animal Model. Cancer Biotherapy and Radiopharmaceuticals, 2005, 20, 231-236.	0.7	28
101	GOT1 Xenografted to Nude Mice: A Unique Model forin VivoStudies on SSTR-Mediated Radiation Therapy of Carcinoid Tumors. Annals of the New York Academy of Sciences, 2004, 1014, 275-279.	1.8	15
102	Importance of Vesicle Proteins in the Diagnosis and Treatment of Neuroendocrine Tumors. Annals of the New York Academy of Sciences, 2004, 1014, 280-283.	1.8	23
103	Biodistribution data from 100 patients i.v. injected with111in-DTPA-D-Phe1-Octreotide. Acta Oncológica, 2004, 43, 436-442.	0.8	30
104	Modelling of metastatic cure after radionuclide therapy: Influence of tumor distribution, cross-irradiation, and variable activity concentration. Medical Physics, 2004, 31, 2628-2635.	1.6	13
105	Chromogranin A as a determinant of midgut carcinoid tumour volume. Regulatory Peptides, 2004, 120, 269-273.	1.9	43
106	Radiolanthanides in nuclear medicine. Metal Ions in Biological Systems, 2004, 42, 77-108.	0.4	2
107	Radiation therapy of small cell lung cancer with 177Lu-DOTA-Tyr3-octreotate in an animal model. Journal of Nuclear Medicine, 2004, 45, 1542-8.	2.8	27
108	Biodistribution of 111in-DTPA-D-Phe1-octreotide in tumor-bearing nude mice: influence of amount injected and route of administration. Nuclear Medicine and Biology, 2003, 30, 253-260.	0.3	23

Eva Forssell-Aronsson

#	Article	IF	CITATIONS
109	Model of metastatic growth valuable for radionuclide therapy. Medical Physics, 2003, 30, 3227-3232.	1.6	22
110	Medical Imaging for Improved Tumour Characterization, Delineation and Treatment Verification. Acta OncolÃ ³ gica, 2002, 41, 604-614.	0.8	18
111	Radiation Therapy Through Activation of Stable Nuclides. Acta OncolÃ ³ gica, 2002, 41, 629-634.	0.8	18
112	Therapy with Radiopharmaceuticals. Acta Oncológica, 2002, 41, 623-628.	0.8	23
113	The magnitude of signal errors introduced by ISIS in quantitative31P MRS. Magnetic Resonance Materials in Physics, Biology, and Medicine, 2002, 14, 30-8.	1.1	2
114	The magnitude of signal errors introduced by ISIS in quantitative 31P MRS. Magnetic Resonance Materials in Physics, Biology, and Medicine, 2002, 14, 30-38.	1.1	3
115	Stunning of iodide transport by (131)I irradiation in cultured thyroid epithelial cells. Journal of Nuclear Medicine, 2002, 43, 828-34.	2.8	42
116	Swedish Cancer Society radiation therapy research investigation. Acta OncolÃ ³ gica, 2002, 41, 596-603.	0.8	0
117	Medical imaging for improved tumour characterization, delineation and treatment verification. Acta Oncológica, 2002, 41, 604-14.	0.8	2
118	Therapy with radiopharmaceuticals. Acta OncolÃ ³ gica, 2002, 41, 623-8.	0.8	5
119	Radiation therapy through activation of stable nuclides. Acta OncolÃ ³ gica, 2002, 41, 629-34.	0.8	2
120	A Transplantable Human Carcinoid as Model for Somatostatin Receptor-Mediated and Amine Transporter-Mediated Radionuclide Uptake. American Journal of Pathology, 2001, 158, 745-755.	1.9	86
121	Similarities and differences between free 211At and 1251â^' transport in porcine thyroid epithelial cells cultured in bicameral chambers. Nuclear Medicine and Biology, 2001, 28, 41-50.	0.3	37
122	Biokinetics of 1111n-DTPA-D-Phe1-octreotide in nude mice transplanted with a human carcinoid tumor. Nuclear Medicine and Biology, 2001, 28, 67-73.	0.3	8
123	Intraoperative tumour detection using 111 In-DTPA- D -Phe 1 -octreotide and a scintillation detector. European Journal of Nuclear Medicine and Molecular Imaging, 2001, 28, 1456-1462.	3.3	28
124	Dosimetric comparison of radionuclides for therapy of somatostatin receptor-expressing tumors. International Journal of Radiation Oncology Biology Physics, 2001, 51, 514-524.	0.4	46
125	Effects of k-space filtering and image interpolation on image fidelity in 1H MRSI. Magnetic Resonance Imaging, 2001, 19, 1227-1234.	1.0	20
126	Differential expression of vesicular monoamine transporter (VMAT) 1 and 2 in gastrointestinal endocrine tumours. Journal of Pathology, 2001, 195, 463-472.	2.1	62

Eva Forssell-Aronsson

#	Article	IF	CITATIONS
127	Extended ISIS sequences insensitive toT1 smearing. Magnetic Resonance in Medicine, 2000, 44, 546-555.	1.9	14
128	114mIn, a candidate for radionuclide therapy: low-energy cyclotron production and labeling of DTPA-D-Phe-octreotide. Nuclear Medicine and Biology, 2000, 27, 183-188.	0.3	28
129	A transplantable human carcinoid as model for somatostatin receptor- and amine transporter mediated radionuclide uptake. Gastroenterology, 2000, 118, A520.	0.6	0
130	Performance of 2D 1H spectroscopic imaging of the brain: some practical considerations regarding the measurement procedure. Magnetic Resonance Imaging, 1999, 17, 919-931.	1.0	7
131	Somatostatin Receptor Subtypes, Octreotide Scintigraphy, and Clinical Response to Octreotide Treatment in Patients with Neuroendocrine Tumors. World Journal of Surgery, 1998, 22, 679-683.	0.8	28
132	Signal profile measurements of single- and double-volume acquisitions with image-selected in vivo spectroscopy for 31P magnetic resonance spectroscopy. Magnetic Resonance Imaging, 1998, 16, 829-837.	1.0	7
133	Castric Carcinoid with Histamine Production, Histamine Transporter and Expression of Somatostatin Receptors. Digestion, 1998, 59, 160-166.	1.2	34
134	Signal profile measurements for evaluation of the volume-selection performance of ISIS. NMR in Biomedicine, 1995, 8, 271-277.	1.6	12